Neuron

Article

SST interneurons facilitate dendritic calcium signaling via tonic activation of α5-GABA receptors

Highlights

- SST interneurons induce tonic activation of α5 GABA receptors in cortical dendrites
- Tonic GABA enhances the opening of voltage-gated calcium channels during dendritic activity
- Tonic GABAergic enhancement of dendritic calcium facilitates synaptic plasticity

Authors

Chiayu Q. Chiu, Thomas M. Morse, Karima AitOuares, ..., Maria-Clemencia Hernandez, Monika Jadi, Michael J. Higley

Correspondence

m.higley@yale.edu

In brief

Chiu et al. found that activation of SST-expressing interneurons induces tonic currents through dendritic α5-containing GABA receptors in pyramidal neurons of the neocortex. Tonic GABAergic hyperpolarization deinactivates dendritic voltage-gated calcium channels, enhancing calcium influx during action potentials. Increased dendritic calcium signaling facilitates calcium- and endocannabinoid-dependent inhibitory synaptic plasticity.

Chiu et al., 2026, Neuron *114*, 1–11
September 16, 2026
https://doi.org/10.1016/j.neuron.2026.04.017

CellPress

Please cite this article in press as: Chiu et al., SST interneurons facilitate dendritic calcium signaling via tonic activation of α5-GABA receptors, Neuron (2026), https://doi.org/10.1016/j.neuron.2026.04.017

Neuron

CellPress
OPEN ACCESS

Article

SST interneurons facilitate dendritic calcium signaling via tonic activation of α5-GABA receptors

Chiayu Q. Chiu,[1,5] Thomas M. Morse,[1,5] Karima AitOuares,[1] Lauren C. Panzera,[1] Paras A. Patel,[1] Francesca Nani,[2] Frederic Knoflach,[2] Maria-Clemencia Hernandez,[2] Monika Jadi,[3] and Michael J. Higley[1,3,4,6,*]

[1]Department of Neuroscience, Yale University, New Haven, CT, USA
[2]Roche Pharmaceutical Research and Early Development, Neuroscience and Rare Diseases (NRD), Roche Innovation Center, Basel, Switzerland
[3]Department of Psychiatry, Yale University, New Haven, CT, USA
[4]Department of Biomedical Engineering, Yale University, New Haven, CT, USA
[5]These authors contributed equally
[6]Lead contact
*Correspondence: m.higley@yale.edu
https://doi.org/10.1016/j.neuron.2026.04.017

SUMMARY

Brain activity is highly regulated by GABAergic activity, which can suppress neuronal excitability and synaptic integration. Tonic GABAergic conductances mediated by distinct receptor subtypes can also inhibit neural activity, although the consequences for dendritic calcium signaling are unclear. Here, we use 2-photon calcium imaging both *ex vivo* and in awake mice to show that α5-$GABA_A$Rs mediate tonic currents in cortical pyramidal neurons that paradoxically enhance action potential-evoked dendritic calcium influx. Experimental and computational data indicate that the increased calcium influx arises via deinactivation of low-threshold voltage-gated channels. Tonic α5-mediated GABAergic currents and dendritic calcium signals are both enhanced by optogenetic activation of somatostatin-expressing interneurons (SST-INs). In addition, α5-mediated GABAergic facilitation of postsynaptic calcium signaling modulates the short-term plasticity of GABAergic transmission at SST-IN synapses. Our results demonstrate unexpected diversity in the function of both SST-INs and GABAergic signaling to influence dendritic activity and synaptic transmission in the cortex.

INTRODUCTION

Neuronal activity in the mammalian brain is strongly shaped by GABAergic signaling, which is mediated by the release of GABA from local interneurons and the subsequent binding to both ionotropic type-A receptors ($GABA_A$Rs) and metabotropic type-B receptors.[1,2] Broadly, the function of GABAergic transmission, and thus GABAergic interneurons, is thought to be inhibitory, providing a brake on neuronal activity.[1,3,4] For example, somatic GABAergic inhibition via fast-spiking, parvalbumin-expressing interneurons can regulate the timing and magnitude of action potential (AP) generation,[5–7] while inhibition from somatostatin-expressing interneurons (SST-INs) can shape synaptic integration and calcium signaling in target dendrites.[8–10] Indeed, these suppressive influences on dendritic calcium are suggested to be critical modulators of synaptic plasticity.[11,12]

In addition to synaptic transmission, GABA can evoke a tonic membrane conductance, which is mediated through $GABA_A$Rs with a subunit composition potentially distinct from that of their synaptic counterparts.[1,13–15] In the hippocampus and neocortex, α4, -5, -6, and δ subunits located extrasynaptically have been most closely linked to tonic GABAergic conductances, contrasting with α1, -2, and γ subunits at conventional synaptic locations.[1,16,17] The source of GABA-activating tonic currents is only partially understood. Prior evidence from hippocampal recordings suggested that GABA released from the same interneurons that mediate synaptic transmission could also support tonic currents,[18] although the specific interneuron subpopulations contributing to tonic signaling remain unknown. Tonic current through $GABA_A$Rs may also be inhibitory, suppressing neuronal output by hyperpolarizing the membrane potential, reducing dendritic propagation of APs, and shunting the integration of synaptic inputs.[1,16,17,19,20] However, there are suggestions that tonic GABA may paradoxically increase neuronal excitability via complex interactions with voltage-gated channels,[20,21] providing competing narratives for the role of GABAergic transmission in shaping neuronal activity. Overall, the relationships between interneuron subpopulations, GABA receptor subtypes, and dendritic calcium signaling are not well

Please cite this article in press as: Chiu et al., SST interneurons facilitate dendritic calcium signaling via tonic activation of α5-GABA receptors, Neuron (2026), https://doi.org/10.1016/j.neuron.2026.04.017

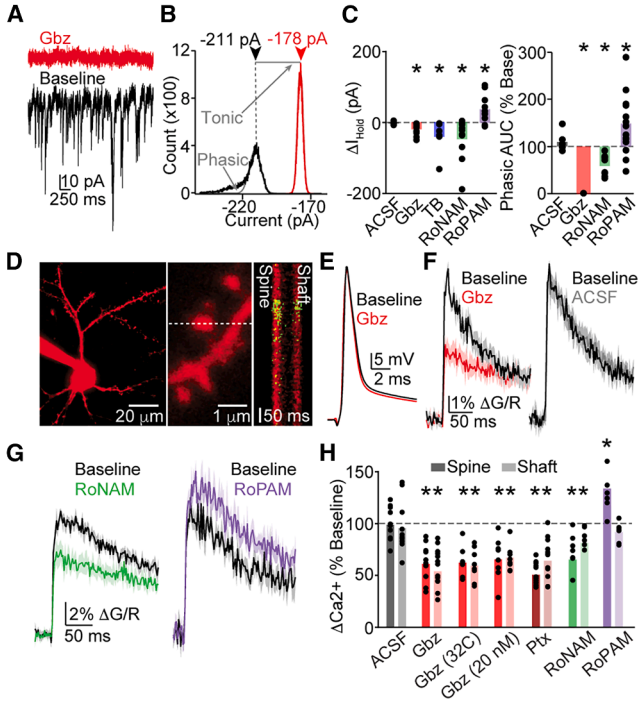

Figure 1. Tonic GABAergic signaling enhances action potential-evoked dendritic calcium transients

(A) Representative voltage-clamp recordings before (black) and after (red) flow-in of 10 μM gabazine (Gbz).

(B) Example histogram of current values during a 3-s recording under control (black) and post-Gbz (red) conditions. Thin lines show the corresponding one-sided Gaussian curve-fits for identifying phasic and tonic currents. The difference in Gaussian peak locations indicates change in tonic current after Gbz application.

(C) Population data (mean and values for individual cells) showing change in currents induced by control ACSF, Gbz, TB21007 (TB), RO4938581 (RoNAM), and RO7015738 (RoPAM). (Left) Change in tonic holding current. (Right) Change in phasic current measured as area under the curve (AUC). * indicates $p < 0.05$ relative to baseline, by Wilcoxon matched-pairs test.

(D) Representative image showing the recording configuration. Layer 2/3 PNs from the mouse prefrontal cortex were filled through the patch pipette with Alexa Fluor 594 and Fluo 5F and imaged using 2-photon laser-scanning microscopy (left). Somatic APs were evoked via somatic current injection, producing brief dendritic calcium transients in spines and neighboring shafts (dashed line indicates line-scan), which are visible as a rise in green fluorescent signal (right).

(E) Average AP waveform under baseline conditions (black) and after flow-in of Gbz (red).

(F) Average AP-evoked spine ΔCa^{2+} under baseline conditions (black) and after flow-in of Gbz (red, left traces) or ACSF (gray, right traces). Lines and shaded regions indicate mean ± SEM.

(G) Average AP-evoked spine ΔCa^{2+} under baseline conditions (black) and after flow-in of RoNAM (left, green) or RoPAM (right, purple). Lines and shaded regions indicate mean ± SEM.

(H) Population data (mean and values for individual spines and dendrites) showing change in ΔCa^{2+} induced by flow-in of ACSF, Gbz, Gbz at 32°C, 20 nM Gbz, picrotoxin (Ptx), RoNAM, or RoPAM. * indicates $p < 0.05$ relative to baseline, by linear mixed-effects model.

See also Figure S1.

understood and may reflect diverse functions of GABAergic circuits in the cortex.

To further investigate how tonic GABAergic currents influence dendritic function, we used 2-photon laser-scanning microscopy to monitor calcium signaling in apical dendrites of layer 2/3 pyramidal neurons (PNs) from the mouse cortex, both *ex vivo* and in awake animals. We found the surprising result that GABA released from SST-INs can evoke tonic current via activation of extrasynaptic α5 subunit-containing receptors that facilitates dendritic calcium influx due to deinactivation of low-threshold voltage-gated calcium channels. Activation of α5-containing receptors also boosts dendritic calcium signals *in vivo* and enhances calcium- and cannabinoid-dependent short-term synaptic plasticity. These results contrast with earlier studies indicating that synaptic transmission from SST-INs can strongly inhibit dendritic calcium signaling,[8–10] suggesting that the functional consequences of GABAergic inputs to PN dendrites may vary depending on the dynamics of the signal (phasic versus tonic) and the receptor subtypes engaged. Overall, our work highlights a novel role for SST-INs and α5 subunit-containing receptors in the neocortex and suggests new avenues for the exploration of GABAergic control of neuronal activity in both health and disease.

RESULTS

To investigate the role of GABAergic signaling, we first performed whole-cell recordings from layer 2/3 PNs in acute slices of mouse frontal cortex. Adapting a method developed by Glykys and Mody,[18] we first measured holding currents using a high-chloride internal solution and in the presence of glutamate receptor blockers, followed by application of the $GABA_AR$ antagonist gabazine (Figure 1A). Under baseline conditions, the distribution of current values was approximately Gaussian with a long left tail, which is consistent with phasic synaptic currents superimposed on a steady tonic current. Gabazine eliminated the phasic events and caused a shift in the mean holding current from −211.0 pA to −178.0 pA (Figures 1B and 1C), with the shift providing a metric of the cell's baseline tonic GABA current.

We repeated similar experiments using the application of either gabazine or agents targeting specific subpopulations of $GABA_ARs$. Gabazine caused a significant change in the tonic current (Wilcoxon test, $n = 10$ cells, $p = 0.002$; Figure 1C). Consistent with prior work suggesting a role for α5 subunit-containing $GABA_ARs$ in mediating tonic currents in cortical neurons,[16,22] the negative allosteric modulators of α5-$GABA_ARs$ TB21007 and RO4938581 (RoNAM)[23] also significantly reduced the tonic membrane current (Wilcoxon matched-pairs test; TB21007, $n = 6$ cells, $p = 0.0312$; RoNAM, $n = 10$ cells, $p = 0.0059$; Figure 1C). Moreover, application of a novel positive allosteric modulator RO7015738 (RoPAM) of α5-$GABA_ARs$ (Figure S1) significantly increased the tonic membrane current (Wilcoxon matched-pairs test, $n = 11$ cells, $p = 0.0049$, Figure 1C). Gabazine also completely abolished phasic events, measured as the area under the curve (Wilcoxon matched-pairs test; $n = 10$, $p = 0.002$). In addition, application of RoNAM and RoPAM produced opposite significant changes in the magnitude of the phasic events (Wilcoxon matched-pairs test; RoNAM, $n = 10$ cells, $p = 0.002$; RoPAM, $n = 11$ cells, $p = 0.0186$). Control experiments applying artificial cerebrospinal fluid (ACSF) did not cause a significant change in either tonic or phasic currents (Wilcoxon matched-pairs test; $n = 6$ cells, $p = 0.8438$ and 0.6875,

Please cite this article in press as: Chiu et al., SST interneurons facilitate dendritic calcium signaling via tonic activation of α5-GABA receptors, Neuron (2026), https://doi.org/10.1016/j.neuron.2026.04.017

respectively). These results indicate that cortical layer 2/3 PNs exhibit spontaneous tonic and phasic GABAergic currents, which are mediated at least partly by α5-containing receptors.

To determine the impact of these currents on dendritic calcium signaling, we filled cells through the patch pipette with internal solution containing a physiological concentration of chloride,[8] the structural indicator Alexa Fluor 594, and the calcium indicator Fluo 5F and imaged apical dendrites using 2-photon microscopy (Figure 1D). Somatic APs that propagated into the dendritic arbor were evoked using brief current injection (1–2 ms, 1–2 nA), and the resulting calcium transients were visualized in single dendritic spines and neighboring dendritic shafts (Figures 1D–1F). Following application of gabazine, we observed a substantial reduction in the magnitude of the AP-evoked calcium transient for both dendritic spines (ΔCa^{2+}, Figures 1F and S1) and neighboring dendritic shafts (Figure 1H). This reduction in ΔCa^{2+} was not caused by rundown, as control experiments applying ACSF did not produce a change in transient amplitude (Figures 1F and 1H). Relative to the pre-drug baseline, 10 μM gabazine (linear mixed-effects model [LME], n = 17 spine/dendrite pairs, p = 0.0002/p = 9.8172e−07), but not ACSF (LME, n = 12 spine/dendrite pairs, p = 0.3605/p = 0.5345) produced a significant reduction in ΔCa^{2+} (Figure 1H). We observed similar results when experiments were carried out at near-physiological temperature (LME, n = 8 spine/dendrite pairs, p = 0.0002/p = 0.0008) and with the distinct $GABA_AR$ blocker picrotoxin (LME, n = 13 spine/dendrite pairs, p = 0.000002/p = 0.0001; Figure 1H). In addition, nanomolar concentrations of gabazine also reduced ΔCa^{2+} (LME, n = 8 spine/dendrite pairs, p = 0.0052/p = 0.0005; Figure 1H). Overall, the magnitudes of calcium signals in spines and dendritic shafts were highly correlated, both before and after drug application (Spearman's R = 0.7267, p < 0.0001; Figure S1), suggesting that similar mechanisms shape activity in both compartments. Application of ACSF, gabazine, or picrotoxin did not produce significant changes in either the input resistance or membrane potential measured at the cell body (Figure S1), suggesting a tonic GABAergic conductance electrotonically distant from the soma. In addition, these experiments revealed no change in the somatic action potential width, amplitude, or peak membrane potential (Figures 1E and S1).

Our whole-cell data suggested a contribution of α5-containing receptors to tonic GABA currents, so we next asked whether dendritic calcium signals were specifically altered by modulation of these receptors. Indeed, the application of RoNAM produced a significant reduction in ΔCa^{2+} (LME, n = 7 spine/dendrite pairs, p = 0.0091/p = 0.0127), while the application of RoPAM produced a significant increase in ΔCa^{2+} for dendritic spines (LME, n = 7, p = 0.0029) though not dendritic shafts (LME, n = 7, p = 0.0987, Figures 1G and 1H). Neither RoNAM nor RoPAM produced changes in somatic input resistance, membrane potential, or AP waveform (Figure S1). Furthermore, RoNAM and RoPAM did not produce significant changes in ΔCa^{2+} when applied after gabazine, suggesting that they do not exert non-GABAergic effects on dendritic signaling (Figure S1). Overall, these combined results indicate that tonic GABAergic currents mediated by α5-containing receptors serve to enhance AP-evoked dendritic calcium influx.

To explore the biophysical mechanisms mediating this paradoxical GABAergic enhancement of dendritic calcium signaling and generate experimentally testable hypotheses, we simulated a biophysically realistic layer 2/3 PN (Figures 2A and S2). Reflecting the expression of diverse voltage-gated calcium channels in cortical neurons, we included both high-threshold ("HVA," N/P/Q/R-like) and low-threshold ("LVA," T-like) conductances. These channel types differ in the dependence of their activation and inactivation dynamics on membrane voltage (Figure S2). We also simulated a tonic GABAergic conductance uniformly distributed in the cell membrane with a reversal potential of −75 mV, which is similar to published data from somatic perforated patch recordings in these cells.[8]

Under control conditions (tonic GABA conductance intact), a somatic AP evoked by current injection propagated through the apical dendrites, producing calcium influx through both HVA and LVA channels (Figure 2A). We then modeled our gabazine experiments by repeating the simulation after removing the tonic GABA conductance. As with the experimental data, this manipulation led to a reduction in calcium influx throughout the dendritic arbor that was primarily driven by decreased LVA-type channel opening following substantial channel inactivation at rest (Figure 2A). Model data revealed a depolarization of the dendritic membrane potential following removal of the tonic GABAergic input (Figure S2). The left-shifted voltage-dependent inactivation curve of the LVA-type channels explained the greater fold-change in their opening versus HVA-type channels (Figure S2) and yielded substantially more reduction in ΔCa^{2+} for models that included only LVA- versus HVA-type channels (Figures 2C and S2).

Exploration of model parameters revealed that the reduction in ΔCa^{2+} following removal of the tonic GABA conductance was enhanced for more distal dendritic compartments and also for somatic depolarization induced by somatic current injection (Figure 2B). In addition, we found that shifting the voltage dependence of LVA channel inactivation (but not activation) to more depolarized potentials dramatically lessened the amount of ΔCa^{2+} reduction (Figures 2C and S2). Finally, we found that the change in dendritic ΔCa^{2+} was not altered by varying the magnitude of current injection used to evoke the AP (Figure S2). Thus, our model results generate multiple clear hypotheses that membrane depolarization, dendritic distance, and involvement of LVA-type calcium channels are critical factors influencing the tonic GABAergic control of dendritic calcium signals.

We next sought to test these hypotheses with additional experimental recordings. First, we measured ΔCa^{2+} in dendritic spines while adjusting the somatic membrane potential via current injection, finding that depolarization induced a significant reduction in AP-evoked calcium influx (Spearman's R = −0.6461, n = 6 spines, p = 0.0006, Figure 2D). We then measured the effect of gabazine on spine ΔCa^{2+} as a function of distance from the cell body, finding significantly greater reduction for more distal locations (Spearman's R = −0.4979, n = 24 spines, p = 0.0133, Figure 2D). We then examined the sensitivity of distinct voltage-gated calcium channel populations to GABAergic influence. Consistent with earlier work in hippocampal PNs, striatal medium spiny neurons, and layer 5 PNs,[24–26] we found that both HVA- and LVA-type channels contribute similarly to AP-evoked calcium

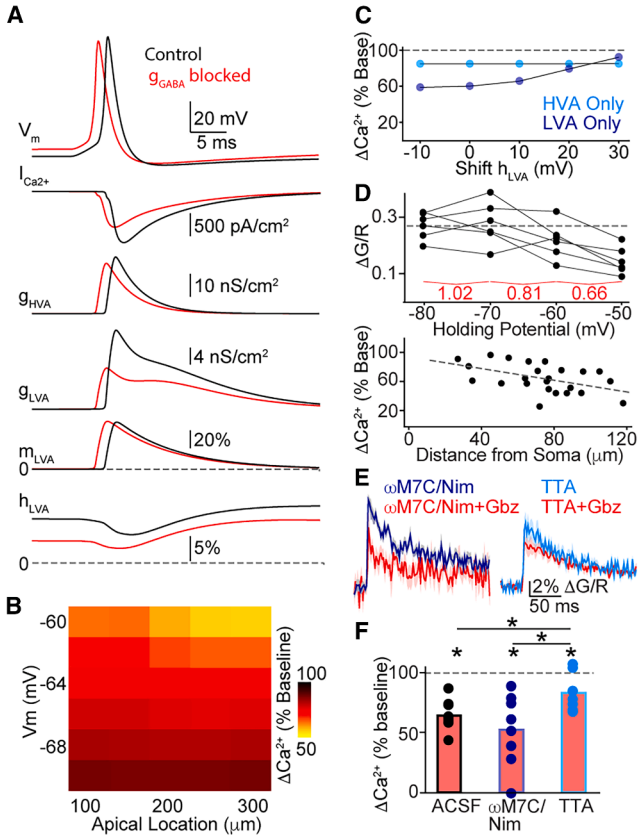

Figure 2. Tonic GABAergic signaling deinactivates dendritic low-threshold voltage-gated calcium channels

(A) Computational modeling data illustrating dendritic voltage (V_m), calcium current (I_{Ca2+}), high- and low-threshold calcium channel conductance (g_{HVA}, g_{LVA}), and low-threshold channel activation and inactivation fraction (m_{LVA}, h_{LVA}) in response to a somatic AP under control conditions (black) and following elimination of tonic GABA conductance (red).

(B) Heatmap of model data showing change in ΔCa^{2+} relative to baseline as a function of dendritic location (distance from soma) and somatic membrane potential caused by removal of the tonic GABA conductance.

(C) Model data showing change in ΔCa^{2+} relative to baseline (200 μm location) after removal of tonic GABA, for varying shifts in the LVA voltage-dependent inactivation curve. Data are for models including only HVA (light blue) or LVA (dark blue) channels.

(D) (Upper graph) Experimental population data (mean values for individual spines) showing the magnitude of ΔCa^{2+} for different values of somatic membrane voltage adjusted via intracellular current injection (top). Numbers indicate fractional change in ΔCa^{2+} for each 10-mV step. (Lower graph) Experimental population data (values for individual spines) showing change in ΔCa^{2+} induced by flow-in of Gbz as a function of dendritic distance from the soma. Dashed line is the linear fit of the values of individual spines.

(E) Average AP-evoked spine calcium transients before (blue) and after (red) application of Gbz. Data are shown for pre-incubation with HVA (left) or LVA (right) channel blockers. Lines and shaded regions indicate mean ± SEM.

(F) Population data (mean and values for individual spines) showing change in ΔCa^{2+} induced by flow-in of Gbz in the presence of ACSF, HVA-type calcium blockade, or LVA-type channel blockade. * indicates $p < 0.05$ relative to baseline, by linear mixed-effects model.

See also Figure S2.

influx. Application of either a combination of N/P/Q- and L-type (HVA) blockers (ω-conotoxin MVIIC and nimodipine) or the T-type (LVA) channel blocker TTA-A2 significantly reduced ΔCa^{2+} (Figure S2), suggesting similar contributions of both channel groups to dendritic calcium influx. We then compared the consequences of applying gabazine to slices pre-treated with either the HVA or LVA blockers. As above, gabazine applied to ACSF-treated slices reduced calcium influx (LME, n = 9 spines, p = 0.0001, Figure 2F). After pre-incubation in ω-conotoxin MVIIC and nimodipine, gabazine also produced a significant reduction in ΔCa^{2+} (LME, n = 8 spines, p = 0.0001) that was modestly though not significantly greater than ACSF-treated slices (LME; p = 0.1894, Figures 2E and 2F). In contrast, after pre-incubation in TTA-A2, gabazine produced a reduction in ΔCa^{2+} (LME, n = 7 spines, p = 0.023) that was significantly less than that seen in the other two groups (LME; versus ACSF, p = 0.0108; versus ω-conotoxin MVIIC and nimodipine, p = 0.0091; Figures 2E and 2F). Further confirming the interaction of LVA-type channels and membrane potential, we found that blocking T-type channels by pre-incubation in TTA-A2 eliminated the voltage dependence of dendritic ΔCa^{2+} (Figure S2). Moreover, modest somatic hyperpolarization (−14.15 ± 2.54 mV) was sufficient to restore control levels of ΔCa^{2+} after application of gabazine (Figure S2). Thus, our experimental data strongly support the hypotheses made by our computational studies, indicating that the control of membrane potential by tonic GABAergic currents can robustly modulate dendritic calcium signals via interaction with T-type (LVA) calcium channels.

The results above indicate that tonic GABAergic currents mediated by α5-containing receptors can act to enhance dendritic calcium signaling in acute brain slice preparations. We next carried out experiments to determine whether similar mechanisms can act in the awake brain. We used viral vectors to co-express the green fluorescent calcium sensor GCaMP6s[27] and the red fluorescent calcium sensor jRCaMP1b[28] in cortical layer 2/3 PNs and carried out multi-planar 2-photon imaging in awake, head-fixed mice.[29,30] To simultaneously image dendritic and somatic dynamics, two differently tuned lasers were coupled into the microscope objective. A 1,064-nm beam was focused to layer 2/3, including PN cell bodies, while a 920-nm beam was independently focused via an electrically tunable lens to a plane within layer 1, including layer 2/3 PN apical dendrites (Figures 3A and S3). This approach enabled us to monitor dendritic (green) and somatic (red) activity at the same time (Figures 3B and 3C). To determine the role of α5-containing $GABA_AR$-mediated signaling on dendritic calcium signaling, we also implanted a guide cannula near the imaging field and followed the same dendritic branches and cell bodies before and after the local infusion of the α5-specific negative modulator TB21007 (Figures 3B and 3C). Similar to our *ex vivo* results, TB21007 induced a significant reduction in the magnitude of calcium events measured in the apical dendrites but did not alter the event rate (Wilcoxon matched-pairs test; amplitude, n = 8 animals, p = 0.0078; interval, n = 8 animals, p = 0.0547; Figure 3D), producing a left shift in the cumulative distribution of dendritic event amplitudes (Figure 3E). In contrast, local administration of TB21007 did not alter either the amplitude or rate of events measured in the cell body (Wilcoxon matched-pairs test; amplitude, n = 5 animals;

Please cite this article in press as: Chiu et al., SST interneurons facilitate dendritic calcium signaling via tonic activation of α5-GABA receptors, Neuron (2026), https://doi.org/10.1016/j.neuron.2026.04.017

CellPress
OPEN ACCESS

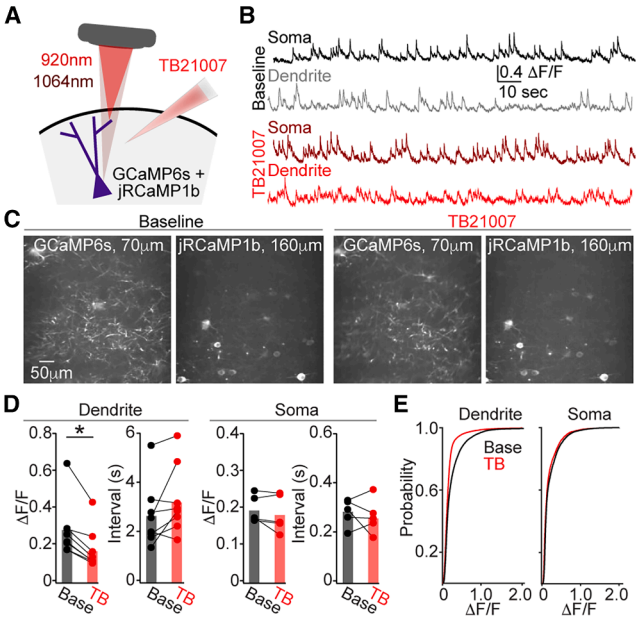

Figure 3. Tonic GABAergic signaling suppresses dendritic calcium signaling *in vivo*

(A) Schematic showing experimental *in vivo* setup for simultaneous two-color dendritic and somatic calcium imaging with local pharmacological infusion.

(B) Example traces of somatic (black, dark red) and dendritic (gray, light red) activity before and after local infusion of TB.

(C) Example fields of view showing dendritic GCaMP6s and somatic jRCaMP1b imaging under baseline conditions and following local infusion of TB. Imaging depth from the pial surface is indicated for each image.

(D) Population data (values for individual animals) showing magnitude (left) and inter-event interval (right) of dendritic calcium transients before (black) and after (red) local TB infusion. * indicates $p < 0.05$ relative to baseline, by Wilcoxon matched-pairs test.

(E) Probability distribution of the magnitude of calcium transients in the dendrites (left) and soma (right) before (black) and after (red) local TB infusion.

See also Figure S3.

$p = 0.4375$; interval, $n = 5$ animals, $p = 0.6250$; Figures 3D and 3E). Local administration of vehicle also did not alter either dendritic or somatic event amplitudes or rates (Figure S3). Finally, we observed similar results for a separate set of experiments in which TB21007 was systemically injected (Figure S3), suggesting broad generalization of these findings. Overall, our results indicate that in the awake brain, α5-containing $GABA_A$Rs can act to enhance dendritic calcium signals with minimal impact on neuronal firing rate.

The sources of GABA in the cortex that contribute to tonic signaling are unknown, although work in the hippocampus suggested that it may arise from local interneurons that also mediate phasic inhibition.[18] We previously found that SST-INs can exert potent, fast inhibitory control over dendritic calcium signals in layer 2/3 PNs.[8] Therefore, we reasoned that these cells may also be well positioned to contribute to tonic GABA signaling in the dendrites. To test this hypothesis, we used a viral vector to express conditional, light-activated excitatory channelrhodopsin2 (ChR2) in SST-INs[31,32] and recorded postsynaptic currents in PNs following a brief burst of light pulses (5 pulses, 50 Hz) delivered through the microscope objective (Figure 4A), consistent with *in vivo* recordings of SST-IN activity.[33] We quantified the tonic current evoked by SST-IN activation in a window either 300–400 ms or 650–750 ms following stimulus onset, a period that falls outside the decay of individual light-evoked synaptic currents (Figure 4A), suggesting a predominance of tonic versus phasic signals. We found that activation of SST-INs reliably induced a tonic current that was significant compared with baseline and decayed with time (Wilcoxon matched-pairs *t* test; $n = 9$ cells; $p = 0.0039$ and $p = 0.0195$ for $Post_{300}$ and $Post_{650}$ windows versus baseline, respectively; $p = 0.0039$ for $Post_{300}$ versus $Post_{650}$; Figure 4B). We also obtained similar results using a longer train of SST-IN stimulation in a distinct cohort of experiments (20 pulses, 20 Hz; Figure S4).

We next characterized the pharmacological profile of the SST-IN-evoked currents. Similar to whole-cell currents, application of RoNAM induced a significant reduction in the magnitude of the evoked tonic current (Wilcoxon matched-pairs *t* test, $n = 7$ cells, $p = 0.0156$, Figure 4C). Consistent with this finding, application of RoNAM, RoPAM, TB21007, and low-concentration gabazine also significantly altered currents evoked by stronger SST-IN stimulation (Figure S4). In contrast, neither RoNAM nor RoPAM significantly altered the amplitude of phasic induced pluripotent stem cells (IPSCs) evoked by SST-IN stimulation, suggesting different complements of receptor subtypes for tonic and phasic currents. Importantly, we found that neither RoNAM nor RoPAM application significantly altered the spontaneous firing rate of SST-INs (Figure S4).

Prior studies suggest that α5-containing receptors mediating tonic currents are located primarily extrasynaptically, where they may be exposed to lower concentrations of GABA than synaptic pools of receptors.[34] To explore this possibility, we took advantage of the low-affinity $GABA_A$R antagonist (1,2,5,6-tetrahydropyridin-4-yl)methylphosphinic acid (TPMPA).[35,36] As expected, application of TPMPA significantly reduced the magnitude of tonic, but not phasic, currents evoked by SST-IN stimulation (Figure S4). We then measured the change in current caused by application of RoNAM after pre-incubation in either TPMPA or control ACSF. We found that RoNAM caused significantly less tonic current reduction in the presence of TPMPA (TPMPA versus ACSF, Mann-Whitney test, $n = 7$, $p = 0.007$, Figure 4C). Thus, our results indicate that SST-IN activity is capable of evoking tonic currents, which are mediated by extrasynaptic α5-containing $GABA_A$Rs.

We investigated whether tonic currents evoked by SST-IN stimulation also influence dendritic calcium signals. We imaged ΔCa^{2+} in dendritic spines in response to individual APs alone and when preceded by SST-IN activation (5 pulses, 50 Hz). We timed the PN AP to fall within the windows of evoked tonic GABA currents as above, finding that activation of SST-INs significantly enhanced the magnitude of dendritic calcium influx (LME, $n = 6$ spines, $p = 0.0001$ and $p = 0.0093$ for $Post_{300}$ and $Post_{650}$, respectively; Figures 4D and 4E). We also observed similar results for stronger SST-IN stimulation (Figure S4). Control experiments showed that light pulses did not alter ΔCa^{2+} when GFP was expressed instead of ChR2, nor when stimulation of SST-INs was carried out in the presence of gabazine (Figures 4D and 4E), suggesting that the actions of SST-INs

Please cite this article in press as: Chiu et al., SST interneurons facilitate dendritic calcium signaling via tonic activation of α5-GABA receptors, Neuron (2026), https://doi.org/10.1016/j.neuron.2026.04.017

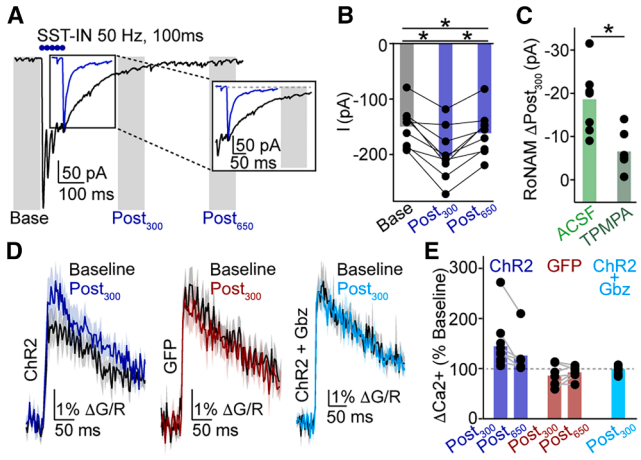

Figure 4. Tonic currents induced by optogenetic activation of SST-INs enhances calcium signaling in PN dendrites

(A) Example single trial whole-cell recording of a layer 2/3 PN during brief optical stimulation of SST-INs (5 pulses at 50 Hz). Shaded regions depict baseline and post-stimulus analysis windows for calculating induced tonic current. Boxed region and inset show superimposed single evoked IPSC (blue), illustrating faster decay rate for synaptic versus tonic current with minimal overlap during analysis window.

(B) Population data (averages and values for individual cells) showing tonic current before and after SST-IN activation for the two indicated post-stimulus windows ($Post_{300}$ and $Post_{650}$). * indicates $p < 0.05$, by Wilcoxon matched-pairs test.

(C) Population data (averages and values for individual cells) showing the effect of RoNAM on SST-IN-induced tonic current in control conditions (ACSF) and in the presence of the low-affinity $GABA_AR$ antagonist TPMPA. * indicates $p < 0.05$, by Wilcoxon matched-pairs test.

(D) (Left) Average AP-evoked calcium transients in L2/3 PNs before (black) and 300-ms after (blue) optical stimulation of SST-INs as in (A) in control ACSF. (Middle) Average calcium transients before (black) and after (maroon) optical illumination of control GFP-expressing SST-INs. (Right) Average calcium transients before (black) and after (light blue) optical stimulation of SST-INs in the presence of Gbz. Lines and shaded regions indicate mean ± SEM.

(E) Population data (mean and values for individual spines) showing change in ΔCa^{2+} relative to baseline for experimental conditions shown in (D). * indicates $p < 0.05$, by linear mixed-effects model.

See also Figure S4.

on dendritic calcium are mediated solely by activation of $GABA_AR$s. Overall, these results indicate that SST-INs are capable of evoking tonic GABAergic currents in layer 2/3 PNs that facilitate dendritic calcium influx.

AP-evoked dendritic calcium influx is linked to various downstream biochemical signaling pathways, including forms of synaptic plasticity such as depolarization-induced suppression of inhibition (DSI). DSI occurs when postsynaptic spiking drives calcium-dependent dendritic endocannabinoid synthesis and subsequent retrograde suppression of GABA release from presynaptic terminals.[37] We hypothesized that tonic GABAergic control of dendritic calcium might therefore modulate this process. To test this possibility, we first established a DSI induction protocol (50 APs at 50 Hz) using brief current pulses through the somatic pipette paired with IPSCs evoked by optogenetic stimulation of SST-INs (Figure 5A). Bursts of somatic spikes produced robust dendritic calcium influx in dendritic spines that was reduced by application of nanomolar gabazine (LME, $n = 6$ spines, $p = 0.0114$, Figures 5B and 5C), which is similar to the suppression of calcium evoked by single spikes. Moreover, PN spike bursts reliably triggered DSI, evident as a significant reduction in the IPSC evoked by SST-IN activation (Wilcoxon matched-pairs test; $n = 8$ cells, $p = 0.0156$, Figures 5D–5F) and an increase in the paired pulse ratio (interstimulus interval = 100 ms; Wilcoxon matched-pairs test; $n = 8$ cells; 0.50 ± 0.02 versus 0.63 ± 0.03 for PPR_{Pre} versus PPR_{Post}, respectively, $p = 0.0068$), which is consistent with a reduced presynaptic release probability. As above, application of nanomolar gabazine caused a modest reduction in SST-IN-evoked IPSC magnitude but also significantly reduced DSI following postsynaptic spike bursts (Wilcoxon matched-pairs test; $n = 8$ cells, $p = 0.0234$, Figures 5D–5F). We obtained similar results using local electrical stimulation instead of optical activation of SST-INs. In addition, we found that DSI was prevented by blocking T-type calcium channels via pre-application of TTA-A (Figure 5G) and also blocked by the cannabinoid receptor inverse agonist AM-251 (Figure S5), suggesting that this form of plasticity requires calcium influx through LVA-type channels and subsequent cannabinoid signaling.

We next explored whether selective modulation of α5-containing $GABA_AR$s could produce similar effects on DSI. Application of RoNAM significantly reduced DSI at synapses formed by SST-INs onto layer 2/3 PNs (Wilcoxon matched-pairs test; $n = 7$, $p = 0.0156$, Figures 5H–5J). In contrast, application of RoPAM significantly increased the amount of DSI observed (Wilcoxon matched-pairs test; $n = 6$, $p = 0.0312$, Figures 5K–5M). Finally, we observed similar effects of RoNAM and RoPAM application on IPSCs evoked by local electrical stimulation (Figure S5), further reinforcing the conclusion that modulation of α5-containing $GABA_AR$s can regulate short-term plasticity of inhibitory synapses.

DISCUSSION

In the present study, we show that tonic GABAergic currents in cortical PNs can enhance dendritic calcium influx during the back-propagation of APs, both in reduced *ex vivo* preparations and in the awake animal. The membrane hyperpolarization caused by tonic GABAergic input deinactivates LVA-type calcium channels as a consequence of their distinct voltage dependence, making more channels available for opening upon depolarization. These tonic currents are mediated by α5-containing $GABA_AR$s, and dendritic calcium influx can be bidirectionally controlled by α5-selective pharmacological modulators. We also find that dendrite-targeting SST-INs provide one possible source of GABA mediating tonic currents, and activation of these interneurons *ex vivo* is sufficient to enhance dendritic calcium signaling. Finally, we show that tonic GABAergic regulation of dendritic calcium influx can modulate the short-term synaptic plasticity of GABAergic inputs, including those formed by SST-INs, providing a novel mechanism for synaptic regulation.[37]

Previous studies demonstrated a role for tonic GABAergic conductances in the steady suppression of neuronal output, which is mediated by both membrane hyperpolarization and the shunting of

Please cite this article in press as: Chiu et al., SST interneurons facilitate dendritic calcium signaling via tonic activation of α5-GABA receptors, Neuron (2026), https://doi.org/10.1016/j.neuron.2026.04.017

CellPress
OPEN ACCESS

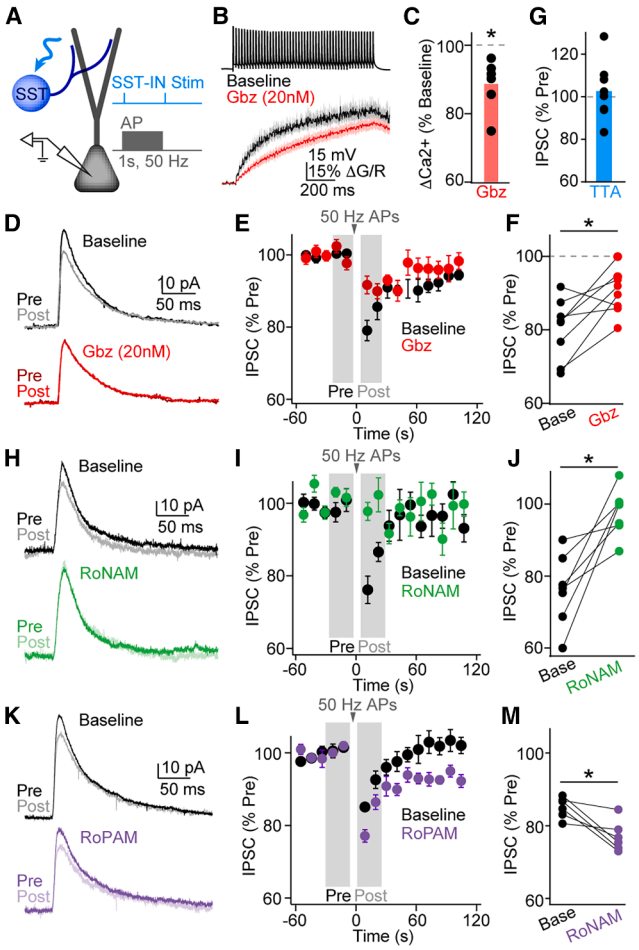

Figure 5. Tonic GABAergic signaling enhances depolarization-induced suppression of inhibition

(A) Schematic showing experimental setup for induction of DSI. Whole-cell recordings of layer 2/3 PNs were paired with optical stimulation of SST-INs. DSI was induced by a brief train of somatic APs.

(B) Average AP burst-evoked calcium transients from dendritic spines before (black) and after (red) application of 20 nM Gbz. Lines and shaded regions indicate mean ± SEM.

(C) Population data (mean and values for individual spines) showing burst-evoked change in ΔCa^{2+} following application of Gbz. * indicates $p < 0.05$, by linear mixed-effects model.

(D) Example IPSCs evoked by optical stimulation of SST-INs recorded before (pre) or after (post) DSI induction for either baseline conditions (black) or after flow-in of 20 nM Gbz (red).

(E) Average (± SEM) time course of normalized SST-IN-evoked IPSC amplitude before and after DSI induction, recorded under baseline conditions (black) and after flow-in of 20 nM Gbz (red). Gray boxes show time intervals for calculating pre- and post-IPSC amplitudes.

(F) Population data (values for individual cells) showing amount of DSI (percentage pre-induction IPSC amplitude) before (black) or after (red) Gbz flow-in. * indicates $p < 0.05$ relative to baseline, by Wilcoxon matched-pairs test.

(G) Population data (mean and values for individual cells) showing amount of DSI in the presence of the T-type calcium channel blocker TTA-A2 (TTA).

(H) Example IPSCs evoked by optical stimulation of SST-INs recorded before (pre) or after (post) DSI induction for either baseline conditions (black) or after flow-in of RoNAM (green).

(I) Average (±SEM) time course of normalized SST-IN-evoked IPSC amplitude before and after DSI induction, recorded under baseline conditions (black) and after flow-in of RoNAM (green).

(J) Population data (values for individual cells) showing amount of DSI (percentage pre-induction IPSC amplitude) before (black) or after RoNAM flow-in. * indicates $p < 0.05$ relative to baseline, by Wilcoxon matched-pairs test.

(K) Example IPSCs evoked by optical stimulation of SST-INs recorded before (pre) or after (post) DSI induction for either baseline conditions (black) or after flow-in of RoPAM (purple).

(L) Average (±SEM) time course of normalized SST-IN-evoked IPSC amplitude before and after DSI induction, recorded under baseline conditions (black) and after flow-in of RoPAM.

(M) Population data (values for individual cells) showing amount of DSI (percentage pre-induction IPSC amplitude) before (black) or after RoPAM flow-in. * indicates $p < 0.05$ relative to baseline, by Wilcoxon matched-pairs test.

See also Figure S5.

synaptic inputs.[1,17] Indeed, α5 subunit-containing $GABA_A$Rs were shown to suppress both the backpropagation of APs in PN dendrites and the opening of NMDA-type glutamate receptors.[19,38] Our present results are not inconsistent with this view, but they suggest that the relationship between membrane potential and voltage-dependent channel gating can add complexity to the consequences of GABAergic signaling. For example, suppression of spike generation or propagation may co-exist with a boosting of calcium influx per spike mediated by a greater fraction of channels in the deinactivated state. The outcome of this complex relationship will certainly depend on a variety of factors, including the instantaneous membrane potential, $GABA_AR$ reversal potential, the specific voltage-dependent dynamics of dendritic calcium channels, and the timing of GABAergic inputs. For example, we and others previously found that triggering an AP immediately after activation of SST-INs or uncaging of GABA, when the inhibitory synaptic conductance is greatest, robustly suppresses both spike- and synaptic-mediated calcium influx through voltage-gated channels and glutamate receptors.[8,10] In contrast, here we find that triggering an AP at a longer interval following SST-IN activation, when GABAergic signaling is dominated by tonic currents, enhances calcium influx. Negative modulation of α5-containing $GABA_A$Rs *in vivo* produced a similar reduction in dendritic calcium signaling without alteration of the neuronal spike rate, suggesting that our findings are not an artifact of reduced brain slice preparations. These results indicate that the relative temporal profile of SST-IN and PN activity may be critical for determining downstream actions on dendritic function. For example, sustained increases in SST-IN firing rates may enhance tonic currents and calcium influx while still allowing individual presynaptic spikes to precisely inhibit dendrites for brief windows of time. In addition, the reversal potential for $GABA_A$Rs in dendritic compartments, as well as their sensitivity to input dynamics, has not been measured. We note that both the present work and prior studies strongly suggest that this value is likely to be hyperpolarized relative to rest.[8] Earlier computational work suggested that activity-dependent increases in intracellular chloride concentrations could diminish the impact of GABAergic inhibition,[39] but this hypothesis has not been confirmed experimentally.

Our results highlight a previously undescribed function for cortical SST-INs, which comprise a heterogeneous group of GABAergic cells that generally contact the dendrites of PNs.[40]

Please cite this article in press as: Chiu et al., SST interneurons facilitate dendritic calcium signaling via tonic activation of α5-GABA receptors, Neuron (2026), https://doi.org/10.1016/j.neuron.2026.04.017

Via their inhibitory actions, SST-INs shape rhythmic network activity, suppress dendritic electrogenesis, and influence dendritic plasticity.[4,9,12,41,42] Several studies have linked SST-INs to neuropsychiatric disorders.[43–46] Indeed, the increased output of SST-INs following genetic ablation of their inhibitory inputs reduces anxiety-like behavior,[43] while reducing SST-IN activity and its modulation of dendritic calcium signaling may contribute to the therapeutic actions of ketamine.[47] These earlier studies have broadly envisioned the primary role of SST-INs as a suppressor of postsynaptic activity. However, our findings suggest that manipulations of SST-INs may also shape tonic GABAergic signaling and produce counterintuitive enhancement of dendritic calcium dynamics and calcium-dependent synaptic plasticity. Importantly, our results do not suggest that SST-INs are the only source of GABA-mediating tonic currents. Several other GABAergic cell types make contacts in the dendritic arbors of PNs, including those expressing vasoactive intestinal peptide and neuron-derived neurotrophic factor.[48,49] Moreover, SST-IN subtypes vary in the structure and potential postsynaptic targeting of their axonal arbors.[50] Thus, whether tonic facilitation of dendritic calcium signaling is IN-type specific remains to be determined.

Our data implicating α5 subunit-containing receptors in generating tonic GABAergic currents and controlling dendritic calcium signaling also add to a growing literature on the roles of these channels in both health and disease.[23,51–53] Previous studies demonstrated the involvement of α5 subunits in tonic inhibitory currents recorded in the hippocampus and neocortex,[16,34] as well as a potential contribution to synaptic currents.[36,54] Pharmacological or genetic manipulation of α5 activity can produce significant modulation of learning and cognitive ability.[55–59] Altered α5 expression has also been linked to neuropsychiatric disorders, and α5 modulators may have antidepressant actions.[60,61] Surprisingly, both negative and positive modulators of α5 subunit-containing receptors have been linked to therapeutic and pro-cognitive effects. One potential resolution for these seemingly disparate findings is that the suppression of spiking activity and the boosting of dendritic calcium signaling may play distinct roles in modifying behavior. Our results suggest that adjunct targeting of voltage-gated calcium channels may provide a novel approach to enhance the behavioral consequences of α5-dependent behavioral modulation. Overall, the present findings indicate the potential for SST-INs acting via α5-containing receptors to play a key role in cortical circuit dynamics, behavior, and neuropsychiatric disease.

Our data suggest that the impact of tonic GABAergic signaling may be spatially heterogeneous across the dendritic arbor, with greater influence on calcium signals at more distal locations. This outcome may reflect heterogeneity in the expression levels of α5 subunits and/or LVA-type calcium channels. Moreover, our results suggest that dendritic depolarization following blockade of tonic GABA conductances is electrotonically distant from the cell body, as we did not observe a significant change in somatic membrane potential. The impact of tonic GABAergic signaling on neuronal function may also be dynamic. Activation of NMDA-type glutamate receptors is implicated in plasticity of both synaptic and extrasynaptic GABAergic synapses,[32,62] which potentially involves the translocation of α5-containing $GABA_A$Rs from extrasynaptic to synaptic locations in the membrane.[59] NMDA-type glutamate receptor signaling, as well as activation of kainate-type glutamate and muscarinic cholinergic receptors may also lead to enhancement of tonic GABA currents in the hippocampus.[63–65] Future studies are necessary to understand more completely the dynamic interaction of GABAergic receptor distribution, GABAergic currents, and dendritic calcium signaling.

In conclusion, our data indicate novel roles for both SST-INs and tonic GABAergic activity via α5-containing receptors in the control of dendritic calcium influx and synaptic plasticity. These findings add to the diverse functions ascribed to this class of dendrite-targeting interneurons and suggest distinct cellular mechanisms by which their activity could influence cortical dynamics and behavior. Indeed, future investigation of links between both SST-INs and α5-$GABA_A$Rs and neuropsychiatric disorders should consider their paradoxical ability to enhance calcium-dependent signaling.

RESOURCE AVAILABILITY

Lead contact

Requests for further information, resources, and reagents should be directed to and will be fulfilled by the lead contact, Michael J. Higley (m.higley@yale.edu).

Materials availability

Requests for reagents used in this study may be made to the lead contact. RoNAM and RoPAM are available upon request directed to M.-C.H. from Roche Pharmaceutical.

Data and code availability

All data are presented in the paper and supplemental information. The computational model is available through the ModelDB repository (http://modeldb.science/2018023; 10.5281/zenodo.19221219). The analysis code is available at https://github.com/cardin-higley-lab/analysisCode; 10.5281/zenodo.19338916. Any additional information required to reanalyze the data reported in this work is available from the lead contact upon request.

ACKNOWLEDGMENTS

The authors wish to thank members of the Higley laboratory and Dr. Jessica A. Cardin for helpful comments during the preparation of this manuscript; the Yale Center for Research Computing for support with the Yale McCleary high performance cluster; Henner Knust for compound synthesis; Christian Miscenic and Marcello Foggetta for cell transfections and membrane preparations; Judith Lengyel, Gregoire Friz, and Maria Karg for cell line generation and radioligand binding assays; and Marie Claire Pflimlin for support with electrophysiological characterization of RO7015738 (RoPAM) selectivity. This work was supported by funding from the NIH(R01MH099045, R01MH113852, and DP1EY033975 to M.J.H. and K01MH097961 to C.Q.C.), from funding agencies in Chile (FONDECYT no. 1171840 and MILENIO PROYECTO P09-022-F, CINV to C.Q.C.), and from Roche Pharmaceutical.

AUTHOR CONTRIBUTIONS

Experiments were conceived and designed by C.Q.C. and M.J.H. Experimental data were acquired by C.Q.C., F.N., L.C.P., P.A.P., and K.A. Modeling data were generated by M.J. and T.M.M. Analyses were carried out by C.Q.C., T.M.M., F.N., P.A.P., and M.J.H. Work was directed and supervised by F.K., M.-C.H., and M.J.H. The manuscript was written by C.Q.C., T.M.M., M.-C.H., and M.J.H.

DECLARATION OF INTERESTS

Parts of this study were supported by Roche Pharmaceutical, which owns the proprietary RO7015738 (RoPAM).

STAR★METHODS

Detailed methods are provided in the online version of this paper and include the following:

- KEY RESOURCES TABLE
- EXPERIMENTAL MODEL AND STUDY PARTICIPANT DETAILS
- METHOD DETAILS
  - Slice preparation
  - AAV virus injection for optogenetic manipulation of SST-INs
  - Electrophysiology and imaging
  - *Ex vivo* pharmacology
  - *In vivo* imaging experiments and pharmacology
  - Radioligand binding and electrophysiological assays of recombinant receptors
  - Computational modeling
- QUANTIFICATION AND STATISTICAL ANALYSIS

SUPPLEMENTAL INFORMATION

Supplemental information can be found online at https://doi.org/10.1016/j.neuron.2026.04.017.

Received: April 16, 2025
Revised: February 13, 2026
Accepted: April 7, 2026

REFERENCES

1. Farrant, M., and Nusser, Z. (2005). Variations on an inhibitory theme: phasic and tonic activation of $GABA_A$ receptors. Nat. Rev. Neurosci. *6*, 215–229. https://doi.org/10.1038/nrn1625.
2. Rose, T.R., and Wickman, K. (2022). Mechanisms and Regulation of Neuronal $GABA_B$ Receptor-Dependent Signaling. Curr. Top. Behav. Neurosci. *52*, 39–79. https://doi.org/10.1007/7854_2020_129.
3. Isaacson, J.S., and Scanziani, M. (2011). How inhibition shapes cortical activity. Neuron *72*, 231–243. https://doi.org/10.1016/j.neuron.2011.09.027.
4. Higley, M.J. (2014). Localized GABAergic inhibition of dendritic Ca^{2+} signalling. Nat. Rev. Neurosci. *15*, 567–572. https://doi.org/10.1038/nrn3803.
5. Pouille, F., and Scanziani, M. (2001). Enforcement of temporal fidelity in pyramidal cells by somatic feed-forward inhibition. Science *293*, 1159–1163. https://doi.org/10.1126/science.1060342.
6. Cruikshank, S.J., Urabe, H., Nurmikko, A.V., and Connors, B.W. (2010). Pathway-specific feedforward circuits between thalamus and neocortex revealed by selective optical stimulation of axons. Neuron *65*, 230–245. https://doi.org/10.1016/j.neuron.2009.12.025.
7. Cardin, J.A., Carlén, M., Meletis, K., Knoblich, U., Zhang, F., Deisseroth, K., Tsai, L.H., and Moore, C.I. (2009). Driving fast-spiking cells induces gamma rhythm and controls sensory responses. Nature *459*, 663–667. https://doi.org/10.1038/nature08002.
8. Chiu, C.Q., Lur, G., Morse, T.M., Carnevale, N.T., Ellis-Davies, G.C., and Higley, M.J. (2013). Compartmentalization of GABAergic inhibition by dendritic spines. Science *340*, 759–762. https://doi.org/10.1126/science.1234274.
9. Murayama, M., Pérez-Garci, E., Nevian, T., Bock, T., Senn, W., and Larkum, M.E. (2009). Dendritic encoding of sensory stimuli controlled by deep cortical interneurons. Nature *457*, 1137–1141. https://doi.org/10.1038/nature07663.
10. Marlin, J.J., and Carter, A.G. (2014). GABA-A receptor inhibition of local calcium signaling in spines and dendrites. J. Neurosci. *34*, 15898–15911. https://doi.org/10.1523/JNEUROSCI.0869-13.2014.
11. Hayama, T., Noguchi, J., Watanabe, S., Takahashi, N., Hayashi-Takagi, A., Ellis-Davies, G.C., Matsuzaki, M., and Kasai, H. (2013). GABA promotes the competitive selection of dendritic spines by controlling local Ca^{2+} signaling. Nat. Neurosci. *16*, 1409–1416. https://doi.org/10.1038/nn.3496.
12. Cichon, J., and Gan, W.B. (2015). Branch-specific dendritic Ca^{2+} spikes cause persistent synaptic plasticity. Nature *520*, 180–185. https://doi.org/10.1038/nature14251.
13. Scimemi, A., Semyanov, A., Sperk, G., Kullmann, D.M., and Walker, M.C. (2005). Multiple and plastic receptors mediate tonic $GABA_A$ receptor currents in the hippocampus. J. Neurosci. *25*, 10016–10024. https://doi.org/10.1523/JNEUROSCI.2520-05.2005.
14. Stell, B.M., and Mody, I. (2002). Receptors with different affinities mediate phasic and tonic $GABA_A$ conductances in hippocampal neurons. J. Neurosci. *22*, RC223. https://doi.org/10.1523/JNEUROSCI.22-10-j0003.2002.
15. Bai, D., Zhu, G., Pennefather, P., Jackson, M.F., MacDonald, J.F., and Orser, B.A. (2001). Distinct functional and pharmacological properties of tonic and quantal inhibitory postsynaptic currents mediated by gamma-aminobutyric acid(A) receptors in hippocampal neurons. Mol. Pharmacol. *59*, 814–824. https://doi.org/10.1124/mol.59.4.814.
16. Jacob, T.C. (2019). Neurobiology and Therapeutic Potential of α5-GABA Type A Receptors. Front. Mol. Neurosci. *12*, 179. https://doi.org/10.3389/fnmol.2019.00179.
17. Lee, V., and Maguire, J. (2014). The impact of tonic $GABA_A$ receptor-mediated inhibition on neuronal excitability varies across brain region and cell type. Front. Neural Circuits *8*, 3. https://doi.org/10.3389/fncir.2014.00003.
18. Glykys, J., and Mody, I. (2007). The main source of ambient GABA responsible for tonic inhibition in the mouse hippocampus. J. Physiol. *582*, 1163–1178. https://doi.org/10.1113/jphysiol.2007.134460.
19. Groen, M.R., Paulsen, O., Pérez-Garci, E., Nevian, T., Wortel, J., Dekker, M.P., Mansvelder, H.D., van Ooyen, A., and Meredith, R.M. (2014). Development of dendritic tonic GABAergic inhibition regulates excitability and plasticity in CA1 pyramidal neurons. J. Neurophysiol. *112*, 287–299. https://doi.org/10.1152/jn.00066.2014.
20. Bryson, A., Hatch, R.J., Zandt, B.J., Rossert, C., Berkovic, S.F., Reid, C.A., Grayden, D.B., Hill, S.L., and Petrou, S. (2020). GABA-mediated tonic inhibition differentially modulates gain in functional subtypes of cortical interneurons. Proc. Natl. Acad. Sci. USA *117*, 3192–3202. https://doi.org/10.1073/pnas.1906369117.
21. Kerr, A.M., and Capogna, M. (2007). Unitary IPSPs enhance hilar mossy cell gain in the rat hippocampus. J. Physiol. *578*, 451–470. https://doi.org/10.1113/jphysiol.2006.121608.
22. Yamada, J., Furukawa, T., Ueno, S., Yamamoto, S., and Fukuda, A. (2007). Molecular basis for the $GABA_A$ receptor-mediated tonic inhibition in rat somatosensory cortex. Cereb. Cortex *17*, 1782–1787. https://doi.org/10.1093/cercor/bhl087.
23. Ballard, T.M., Knoflach, F., Prinssen, E., Borroni, E., Vivian, J.A., Basile, J., Gasser, R., Moreau, J.L., Wettstein, J.G., Buettelmann, B., et al. (2009). RO4938581, a novel cognitive enhancer acting at $GABA_A$ alpha5 subunit-containing receptors. Psychopharmacol. (Berl.) *202*, 207–223. https://doi.org/10.1007/s00213-008-1357-7.
24. Chalifoux, J.R., and Carter, A.G. (2011). $GABA_B$ receptor modulation of voltage-sensitive calcium channels in spines and dendrites. J. Neurosci. *31*, 4221–4232. https://doi.org/10.1523/JNEUROSCI.4561-10.2011.
25. Bloodgood, B.L., and Sabatini, B.L. (2009). NMDA Receptor-Mediated Calcium Transients in Dendritic Spines. In Biology of the NMDA Receptor, A.M. Van Dongen, ed., ed. (CRC Press/Taylor & Francis), pp. 247–262.

26. Higley, M.J., and Sabatini, B.L. (2010). Competitive regulation of synaptic Ca^{2+} influx by D2 dopamine and A2A adenosine receptors. Nat. Neurosci. *13*, 958–966. https://doi.org/10.1038/nn.2592.

27. Chen, T.W., Wardill, T.J., Sun, Y., Pulver, S.R., Renninger, S.L., Baohan, A., Schreiter, E.R., Kerr, R.A., Orger, M.B., Jayaraman, V., et al. (2013). Ultrasensitive fluorescent proteins for imaging neuronal activity. Nature *499*, 295–300. https://doi.org/10.1038/nature12354.

28. Dana, H., Mohar, B., Sun, Y., Narayan, S., Gordus, A., Hasseman, J.P., Tsegaye, G., Holt, G.T., Hu, A., Walpita, D., et al. (2016). Sensitive red protein calcium indicators for imaging neural activity. eLife *5*, e12727. https://doi.org/10.7554/eLife.12727.

29. Puścian, A., Benisty, H., and Higley, M.J. (2020). NMDAR-Dependent Emergence of Behavioral Representation in Primary Visual Cortex. Cell Rep. *32*, 107970. https://doi.org/10.1016/j.celrep.2020.107970.

30. Tang, L., and Higley, M.J. (2020). Layer 5 Circuits in V1 Differentially Control Visuomotor Behavior. Neuron *105*, 346–354.e5. https://doi.org/10.1016/j.neuron.2019.10.014.

31. Boyden, E.S., Zhang, F., Bamberg, E., Nagel, G., and Deisseroth, K. (2005). Millisecond-timescale, genetically targeted optical control of neural activity. Nat. Neurosci. *8*, 1263–1268. https://doi.org/10.1038/nn1525.

32. Chiu, C.Q., Martenson, J.S., Yamazaki, M., Natsume, R., Sakimura, K., Tomita, S., Tavalin, S.J., and Higley, M.J. (2018). Input-Specific NMDAR-Dependent Potentiation of Dendritic GABAergic Inhibition. Neuron *97*, 368–377.e3. https://doi.org/10.1016/j.neuron.2017.12.032.

33. Polack, P.O., Friedman, J., and Golshani, P. (2013). Cellular mechanisms of brain state-dependent gain modulation in visual cortex. Nat. Neurosci. *16*, 1331–1339. https://doi.org/10.1038/nn.3464.

34. Caraiscos, V.B., Elliott, E.M., You-Ten, K.E., Cheng, V.Y., Belelli, D., Newell, J.G., Jackson, M.F., Lambert, J.J., Rosahl, T.W., Wafford, K.A., et al. (2004). Tonic inhibition in mouse hippocampal CA1 pyramidal neurons is mediated by alpha5 subunit-containing gamma-aminobutyric acid type A receptors. Proc. Natl. Acad. Sci. USA *101*, 3662–3667. https://doi.org/10.1073/pnas.0307231101.

35. Barberis, A., Petrini, E.M., and Cherubini, E. (2004). Presynaptic source of quantal size variability at GABAergic synapses in rat hippocampal neurons in culture. Eur. J. Neurosci. *20*, 1803–1810. https://doi.org/10.1111/j.1460-9568.2004.03624.x.

36. Szabadics, J., Tamás, G., and Soltesz, I. (2007). Different transmitter transients underlie presynaptic cell type specificity of GABAA,slow and GABAA,fast. Proc. Natl. Acad. Sci. USA *104*, 14831–14836. https://doi.org/10.1073/pnas.0707204104.

37. Chevaleyre, V., Takahashi, K.A., and Castillo, P.E. (2006). Endocannabinoid-mediated synaptic plasticity in the CNS. Annu. Rev. Neurosci. *29*, 37–76. https://doi.org/10.1146/annurev.neuro.29.051605.112834.

38. Schulz, J.M., Knoflach, F., Hernandez, M.C., and Bischofberger, J. (2018). Dendrite-targeting interneurons control synaptic NMDA-receptor activation via nonlinear α5-$GABA_A$ receptors. Nat. Commun. *9*, 3576. https://doi.org/10.1038/s41467-018-06004-8.

39. Qian, N., and Sejnowski, T.J. (1990). When is an inhibitory synapse effective? Proc. Natl. Acad. Sci. USA *87*, 8145–8149. https://doi.org/10.1073/pnas.87.20.8145.

40. Wu, S.J., Sevier, E., Dwivedi, D., Saldi, G.A., Hairston, A., Yu, S., Abbott, L., Choi, D.H., Sherer, M., Qiu, Y., et al. (2023). Cortical somatostatin interneuron subtypes form cell-type-specific circuits. Neuron *111*, 2675–2692.e9. https://doi.org/10.1016/j.neuron.2023.05.032.

41. Riedemann, T. (2019). Diversity and Function of Somatostatin-Expressing Interneurons in the Cerebral Cortex. Int. J. Mol. Sci. *20*, 2952. https://doi.org/10.3390/ijms20122952.

42. Veit, J., Hakim, R., Jadi, M.P., Sejnowski, T.J., and Adesnik, H. (2017). Cortical gamma band synchronization through somatostatin interneurons. Nat. Neurosci. *20*, 951–959. https://doi.org/10.1038/nn.4562.

43. Fuchs, T., Jefferson, S.J., Hooper, A., Yee, P.P., Maguire, J., and Luscher, B. (2017). Disinhibition of somatostatin-positive interneurons by deletion of postsynaptic $GABA_A$ receptors. Mol. Psychiatry *22*, 787. https://doi.org/10.1038/mp.2017.110.

44. Lewis, D.A., and Hashimoto, T. (2007). Deciphering the disease process of schizophrenia: the contribution of cortical GABA neurons. Int. Rev. Neurobiol. *78*, 109–131. https://doi.org/10.1016/S0074-7742(06)78004-7.

45. Fee, C., Prevot, T.D., Misquitta, K., Knutson, D.E., Li, G., Mondal, P., Cook, J.M., Banasr, M., and Sibille, E. (2021). Behavioral Deficits Induced by Somatostatin-Positive GABA Neuron Silencing Are Rescued by Alpha 5 GABA-A Receptor Potentiation. Int. J. Neuropsychopharmacol. *24*, 505–518. https://doi.org/10.1093/ijnp/pyab002.

46. Tomoda, T., Sumitomo, A., Newton, D., and Sibille, E. (2022). Molecular origin of somatostatin-positive neuron vulnerability. Mol. Psychiatry *27*, 2304–2314. https://doi.org/10.1038/s41380-022-01463-4.

47. Ali, F., Gerhard, D.M., Sweasy, K., Pothula, S., Pittenger, C., Duman, R.S., and Kwan, A.C. (2020). Ketamine disinhibits dendrites and enhances calcium signals in prefrontal dendritic spines. Nat. Commun. *11*, 72. https://doi.org/10.1038/s41467-019-13809-8.

48. Zhou, X., Rickmann, M., Hafner, G., and Staiger, J.F. (2017). Subcellular Targeting of VIP Boutons in Mouse Barrel Cortex is Layer-Dependent and not Restricted to Interneurons. Cereb. Cortex *27*, 5353–5368. https://doi.org/10.1093/cercor/bhx220.

49. Cohen-Kashi Malina, K., Tsivourakis, E., Kushinsky, D., Apelblat, D., Shtiglitz, S., Zohar, E., Sokoletsky, M., Tasaka, G.I., Mizrahi, A., Lampl, I., and Spiegel, I. (2021). NDNF interneurons in layer 1 gain-modulate whole cortical columns according to an animal's behavioral state. Neuron *109*, 2150–2164.e5. https://doi.org/10.1016/j.neuron.2021.05.001.

50. Urban-Ciecko, J., and Barth, A.L. (2016). Somatostatin-expressing neurons in cortical networks. Nat. Rev. Neurosci. *17*, 401–409. https://doi.org/10.1038/nrn.2016.53.

51. Engin, E., Benham, R.S., and Rudolph, U. (2018). An Emerging Circuit Pharmacology of $GABA_A$ Receptors. Trends Pharmacol. Sci. *39*, 710–732. https://doi.org/10.1016/j.tips.2018.04.003.

52. Hauser, J., Rudolph, U., Keist, R., Möhler, H., Feldon, J., and Yee, B.K. (2005). Hippocampal α5 subunit-containing $GABA_A$ receptors modulate the expression of prepulse inhibition. Mol. Psychiatry *10*, 201–207. https://doi.org/10.1038/sj.mp.4001554.

53. Paine, T.A., Chang, S., and Poyle, R. (2020). Contribution of $GABA_A$ receptor subunits to attention and social behavior. Behav. Brain Res. *378*, 112261. https://doi.org/10.1016/j.bbr.2019.112261.

54. Ali, A.B., and Thomson, A.M. (2008). Synaptic α5 subunit-containing $GABA_A$ receptors mediate IPSPs elicited by dendrite-preferring cells in rat neocortex. Cereb. Cortex *18*, 1260–1271. https://doi.org/10.1093/cercor/bhm160.

55. Braudeau, J., Delatour, B., Duchon, A., Pereira, P.L., Dauphinot, L., de Chaumont, F., Olivo-Marin, J.C., Dodd, R.H., Hérault, Y., and Potier, M.C. (2011). Specific targeting of the GABA-A receptor α5 subtype by a selective inverse agonist restores cognitive deficits in Down syndrome mice. J. Psychopharmacol. *25*, 1030–1042. https://doi.org/10.1177/0269881111405366.

56. Collinson, N., Kuenzi, F.M., Jarolimek, W., Maubach, K.A., Cothliff, R., Sur, C., Smith, A., Otu, F.M., Howell, O., Atack, J.R., et al. (2002). Enhanced learning and memory and altered GABAergic synaptic transmission in mice lacking the α5 subunit of the $GABA_A$ receptor. J. Neurosci. *22*, 5572–5580. https://doi.org/10.1523/JNEUROSCI.22-13-05572.2002.

57. Magnin, E., Francavilla, R., Amalyan, S., Gervais, E., David, L.S., Luo, X., and Topolnik, L. (2019). Input-Specific Synaptic Location and Function of the α5 $GABA_A$ Receptor Subunit in the Mouse CA1 Hippocampal Neurons. J. Neurosci. *39*, 788–801. https://doi.org/10.1523/JNEUROSCI.0567-18.2018.

58. Donegan, J.J., Boley, A.M., Yamaguchi, J., Toney, G.M., and Lodge, D.J. (2019). Modulation of extrasynaptic GABAA alpha 5 receptors in the ventral hippocampus normalizes physiological and behavioral deficits in

a circuit specific manner. Nat. Commun. *10*, 2819. https://doi.org/10.1038/s41467-019-10800-1.

59. Davenport, C.M., Rajappa, R., Katchan, L., Taylor, C.R., Tsai, M.C., Smith, C.M., de Jong, J.W., Arnold, D.B., Lammel, S., and Kramer, R.H. (2021). Relocation of an Extrasynaptic $GABA_A$ Receptor to Inhibitory Synapses Freezes Excitatory Synaptic Strength and Preserves Memory. Neuron *109*, 123–134.e4. https://doi.org/10.1016/j.neuron.2020.09.037.
60. Carreno, F.R., Lodge, D.J., and Frazer, A. (2020). Ketamine: Leading us into the future for development of antidepressants. Behav. Brain Res. *383*, 112532. https://doi.org/10.1016/j.bbr.2020.112532.
61. Prevot, T.D., Li, G., Cook, J.M., and Sibille, E. (2019). Insight into Novel Treatment for Cognitive Dysfunctions across Disorders. ACS Chem. Neurosci. *10*, 2088–2090. https://doi.org/10.1021/acschemneuro.9b00148.
62. Gu, X., Zhou, L., and Lu, W. (2016). An NMDA Receptor-Dependent Mechanism Underlies Inhibitory Synapse Development. Cell Rep. *14*, 471–478. https://doi.org/10.1016/j.celrep.2015.12.061.
63. Wyroślak, M., Lebida, K., and Mozrzymas, J.W. (2021). Induction of Inhibitory Synaptic Plasticity Enhances Tonic Current by Increasing the Content of α5-Subunit Containing $GABA_A$ Receptors in Hippocampal Pyramidal Neurons. Neuroscience *467*, 39–46. https://doi.org/10.1016/j.neuroscience.2021.05.020.
64. Jiang, L., Kang, D., and Kang, J. (2015). Potentiation of tonic GABAergic inhibition by activation of postsynaptic kainate receptors. Neuroscience *298*, 448–454. https://doi.org/10.1016/j.neuroscience.2015.04.043.
65. Domínguez, S., Fernández de Sevilla, D., and Buño, W. (2016). Muscarinic Long-Term Enhancement of Tonic and Phasic $GABA_A$ Inhibition in Rat CA1 Pyramidal Neurons. Front. Cell. Neurosci. *10*, 244. https://doi.org/10.3389/fncel.2016.00244.
66. Taniguchi, H., He, M., Wu, P., Kim, S., Paik, R., Sugino, K., Kvitsiani, D., Fu, Y., Lu, J., Lin, Y., et al. (2011). A resource of Cre driver lines for genetic targeting of GABAergic neurons in cerebral cortex. Neuron *71*, 995–1013. https://doi.org/10.1016/j.neuron.2011.07.026.
67. Pologruto, T.A., Sabatini, B.L., and Svoboda, K. (2003). ScanImage: flexible software for operating laser scanning microscopes. Biomed. Eng. OnLine *2*, 13. https://doi.org/10.1186/1475-925X-2-13.
68. Hines, M.L., and Carnevale, N.T. (1997). The NEURON simulation environment. Neural Comput. *9*, 1179–1209. https://doi.org/10.1162/neco.1997.9.6.1179.
69. Iascone, D.M., Li, Y., Sümbül, U., Doron, M., Chen, H., Andreu, V., Goudy, F., Blockus, H., Abbott, L.F., Segev, I., et al. (2020). Whole-Neuron Synaptic Mapping Reveals Spatially Precise Excitatory/Inhibitory Balance Limiting Dendritic and Somatic Spiking. Neuron *106*, 566–578.e8. https://doi.org/10.1016/j.neuron.2020.02.015.
70. Avery, R.B., and Johnston, D. (1996). Multiple channel types contribute to the low-voltage-activated calcium current in hippocampal CA3 pyramidal neurons. J. Neurosci. *16*, 5567–5582. https://doi.org/10.1523/JNEUROSCI.16-18-05567.1996.
71. Foehring, R.C., Mermelstein, P.G., Song, W.J., Ulrich, S., and Surmeier, D.J. (2000). Unique properties of R-type calcium currents in neocortical and neostriatal neurons. J. Neurophysiol. *84*, 2225–2236. https://doi.org/10.1152/jn.2000.84.5.2225.
72. Grunditz, A., Holbro, N., Tian, L., Zuo, Y., and Oertner, T.G. (2008). Spine neck plasticity controls postsynaptic calcium signals through electrical compartmentalization. J. Neurosci. *28*, 13457–13466. https://doi.org/10.1523/JNEUROSCI.2702-08.2008.
73. Giovannucci, A., Friedrich, J., Gunn, P., Kalfon, J., Brown, B.L., Koay, S.A., Taxidis, J., Najafi, F., Gauthier, J.L., Zhou, P., et al. (2019). CaImAn an open source tool for scalable calcium imaging data analysis. eLife *8*, e38173. https://doi.org/10.7554/eLife.38173.

Please cite this article in press as: Chiu et al., SST interneurons facilitate dendritic calcium signaling via tonic activation of α5-GABA receptors, Neuron (2026), https://doi.org/10.1016/j.neuron.2026.04.017

STAR★METHODS

KEY RESOURCES TABLE

REAGENT or RESOURCE	SOURCE	IDENTIFIER
Bacterial and virus strains		
AAV5-EF1a-DIO-hChR2(H134R)-EYFP	Boyden et al.[31]	Addgene 20298
AAV9-Syn-GCaMP6s	Chen et al.[27]	Addgene 100845
AAV9-Syn-jRCaMP1b	Dana et al.[28]	Addgene 100851
Chemicals, peptides, and recombinant proteins		
NBQX	Tocris	#0190
R-CPP	Tocris	#0247
CGP 55845 hydrochloride	Tocris	#1248
SR 95531 hydrobromide (Gabazine)	Tocris	#1262
TB 21007	Tocris	#2905
RO4938581 (RoNAM)	Hoffman-La Roche	N/A
RO7015738 (RoPAM)	Hoffman-La Roche	N/A
Picrotoxin	Tocris	#1128
TPMPA	Tocris	#1040
ω-Conotoxin MVIIC	Tocris	#1084
Nimodipine	Tocris	#0600
TTA-A2	Bruce Bean, Harvard	N/A
AM251	Tocris	#1117
Diazepam	Tocris	#2805
GABA	Tocris	#0344
Midazolam hydrochloride	Tocris	#2832
Retro-inverso dioleoylmelittin (riDOM)	Hoffman-La Roche	N/A
Polyethylenimine (PEI)	Hoffman-La Roche	N/A
Experimental models: Cell lines		
HEK293-F cells	ThermoFisher	N/A
Experimental models: Organisms/strains		
Mouse: SOM-Cre ($Sst^{tm2.1(cre)Zjh}$/J)	The Jackson Laboratory	RRID: IMSR_JAX:013044
Recombinant DNA		
Plasmids for $GABA_AR$ α, β, γ-subunit cDNA	Hoffman-La Roche	N/A
pcDNA3.1 vector	Invitrogen	N/A
Software and algorithms		
Biophysically realistic model in Neuron environment	ModelDB	2018023
ImageJ	NIH	https://imagej.net/software/fiji/
Analysis code (CalmAn and Python)	GitHub	cardin-higley-lab
MATLAB fitlme	MathWorks	https://www.mathworks.com/help/stats/fitlme.html
Other		
Retro-inverso dioleoylmelittin (riDOM)	Hoffman-La Roche	N/A
Polyethylenimine (PEI)	Hoffman-La Roche	N/A

EXPERIMENTAL MODEL AND STUDY PARTICIPANT DETAILS

All animal handling was performed according to the Yale Institutional Animal Care and Use Committee and federal guidelines. Experiments were carried out using young adult (aged P25-P60 for slice experiments, P60-P90 for *in vivo* experiments) wild-type

Please cite this article in press as: Chiu et al., SST interneurons facilitate dendritic calcium signaling via tonic activation of α5-GABA receptors, Neuron (2026), https://doi.org/10.1016/j.neuron.2026.04.017

C57/Bl6 or SST-Cre[66] mice of both sexes. Mice were group housed under standard conditions and allocated randomly for each experiment.

METHOD DETAILS

Slice preparation

Acute slices of the prefrontal cortex were prepared from wild-type C57/Bl6 or SST-Cre mice at postnatal day 25-60. Briefly, isoflurane-anesthetized mice were decapitated and 300 μm coronal slices were cut in ice-cold external solution containing (in mM): 100 choline, 25 $NaHCO_3$, 1.25 NaH_2PO_4, 2.5 KCl, 7 $MgCl_2$, 0.5 $CaCl_2$, 15 glucose, 11.6 sodium ascorbate and 3.1 sodium pyruvate, bubbled with 95% O_2 and 5% CO_2. Slices containing prelimbic and infralimbic regions were then transferred to artificial cerebrospinal fluid (ACSF) containing (in mM): 127 NaCl, 25 $NaHCO_3$, 1.25 NaH_2PO_4, 2.5 KCl, 1 $MgCl_2$, 2 $CaCl_2$ and 15 glucose, bubbled with 95% O_2 and 5% CO_2. After an incubation period of 30 min at 34°C, the slices were maintained at 22–24°C for at least 20 min before use.

AAV virus injection for optogenetic manipulation of SST-INs

To optically stimulate SST-INs, we conditionally expressed the light-activated cationic channel channelrhodopsin2 (ChR2)[31] in a SST-Cre transgenic mouse line,[66] mice were anesthetized with 1–2% isoflurane and maintained at 37°C. A small burr hole was made through the skull followed by injection into the superficial cortex with 500 nl of AAV5-Ef1a-Flex-ChR2-YFP ($3.8x10^{12}$ vg/ml, Addgene #20298). Mice were sacrificed 18-25 days post-injection for slice preparation.

Electrophysiology and imaging

Experiments were conducted at room temperature (~22°C) or near-physiological temperature (32°C) where noted in a submersion-type recording chamber. Whole-cell recordings were obtained from layer 2/3 pyramidal cells (200-300 μm from the pial surface) identified with video-infrared/differential interference contrast. Glass electrodes (3.2–3.8 MΩ) were filled with different internal solutions for various experiments, noted in the text. For current clamp studies, the internal contained (in mM): 135 $KMeSO_3$, 10 HEPES, 4 $MgCl_2$, 4 Na_2ATP, 0.4 NaGTP and 10 sodium creatine phosphate, adjusted to pH 7.3 with KOH. In addition, red-fluorescent Alexa Fluor-594 (10 μM) and green-fluorescent Fluo-5F (300 μM) were included in the pipette solution to visualize cell morphology and changes of intracellular calcium concentration, respectively. For voltage clamp studies, the internal contained (in mM) 135 CsGluconate, 10 HEPES, 4 $MgCl_2$, 4 Na_2ATP, 0.4 NaGTP, 10 sodium creatine phosphate, and 1 EGTA adjusted to pH 7.3 with CsOH. For some experiments, a high chloride (100 mM) internal was used, resulting in inward GABAergic currents. For voltage clamp experiments, the series resistance was kept <25Ω, and experiments were discarded if this value changed more than 20% during the recording. Electrophysiological recordings were made using a Multiclamp 700B amplifier, filtered at 4 kHz and digitized at 10 kHz.

For imaging, neurons were filled via the recording pipette for at least 15 min before collecting data. The membrane potential was standardized across experiments to -60 mV (unless otherwise stated), and action potentials were evoked using a brief depolarizing current pulse (1-2 ms, 1-2 nA). Imaging was performed with a custom-built microscope. Fluorophores were excited using 840 nm light from a titanium-sapphire laser (Ultra-2, Coherent). Emitted green and red photons were separated and collected by photomultiplier tubes. Imaged spines were located along secondary and tertiary branches of the apical dendrite, defined as the largest branch emerging from the cell body in the direction of the brain surface, approximately 30-120 μm from the soma. AP-evoked transients were collected during 500 Hz line scans across a spine and the neighboring dendritic shaft. Reference frame scans were taken between each acquisition to correct for small spatial drift of the preparation over time. Calcium signals were quantified as increases in green fluorescence from baseline normalized to the average red fluorescence (ΔG/R). Data were acquired using National Instruments data acquisition boards and ScanImage software.[67]

For optogenetic stimulation of SST-INs, a blue LED (CoolLED) was coupled to the microscope and directed through the objective. Brief pulses (1 ms, 2 mW at the sample) of light reliably evoked postsynaptic currents. For electrical stimulation of inhibitory synaptic currents, we placed a glass theta stimulating electrode in layer 1 < 100 μm from the recorded cell and used brief (0.1 ms) pulses to evoke IPSCs every 6 s. DSI was induced with action potential bursts evoked by somatic current injection delivered at 50 Hz for 1 s.

Ex vivo pharmacology

For most experiments, the ACSF included (in μM) 10 NBQX and 3 CGP-55845 to block AMPA-type glutamate receptors and $GABA_B$ receptors, respectively. $GABA_B$ receptors were left intact for experiments in Figures 4 and S2G. For calcium imaging experiments, the ACSF also included 10 μM R-CPP to block NMDA-type glutamate receptors. For a subset of experiments (see text), the ACSF included (in μM): 50 picrotoxin, 10 or 0.02 gabazine, 1 TTA-A2, 3 nimodipine, 1 ω-conotoxin MVIIC, 10 RO4938581 (RoNAM), 0.01 TB21007, 1 RO7015738 1 (RoPAM), 100 TPMPA or 2 DHPG. TTA-A2 was a gift from Bruce Bean, Harvard Medical School. RO4938581 and RO7015738 were synthesized and contributed by Hoffman-La Roche (Basel, Switzerland). All other compounds were purchased from Tocris. Compounds were dissolved in water except for picrotoxin and nimodipine, dissolved in 0.05% ethanol, and RoNAM and RoPAM, dissolved in 0.05% DMSO.

Please cite this article in press as: Chiu et al., SST interneurons facilitate dendritic calcium signaling via tonic activation of α5-GABA receptors, Neuron (2026), https://doi.org/10.1016/j.neuron.2026.04.017

In vivo imaging experiments and pharmacology

Mice were anesthetized with 1–2% isoflurane and maintained at 37°C. For virus injection and headpost implantation, the skin and fascia were retracted and the skull was cleaned with sterile saline and lightly scored with a scalpel. A small burr hole was drilled through the skull and 500 nl of a 1:1 mixture of AAV9-Syn-GCaMP6s ($2.8x10^{12}$ vg/ml, Addgene #100845) and AAV9-Syn-jRCaMP1b ($2.4x10^{12}$ vg/ml, Addgene #100851) was injected into the superficial neocortex (100-200 μm from the pial surface), resulting in labeling of primarily layer 2/3 pyramidal neurons. Next, a custom titanium headpost was secured using dental cement. A ~3×3 mm craniotomy was then performed over the injected region, leaving the dura intact. For local perfusion experiments, a stainless-steel cannula was also implanted adjacent to the cranial window, with the guide tip inserted to gently contact the dura. A dual-layer glass window composed of a 3×3 mm square coverslip and a 5-mm square coverslip adhered with UV-cured glue (Norland Products) was mounted over the craniotomy and sealed using cyanoacrylate glue. After surgery, mice received postoperative analgesia and were allowed to recover for a minimum of 2 weeks before imaging.

For *in vivo* imaging, mice were head-fixed and allowed to run freely on a cylindrical wheel placed underneath the microscope objective. Imaging was performed using a MOM two-photon microscope (Sutter Instruments) equipped with a 16x, 0.8 NA objective (Nikon). GCaMP6s was excited using a titanium-sapphire laser (Mai-Tai eHP DeepSee, Spectra-Physics) tuned to 920 nm. jRCaMP1b was excited using a fixed-wavelength laser (Fidelity2, Coherent) emitting at 1064 nm. Green and red emitted fluorescence was collected separately and detected with GaAsP photomultiplier tubes (Hamamatsu). Two imaging planes were collected simultaneously by first focusing on the cell body layer and then moving the focal plane of the 920 nm beam to a more superficial depth using an electrically tunable lens placed in the optical path. Images were collected at 256 × 256 resolution and 30 Hz frame rate using a galvo-resonant scan system controlled by ScanImage (Vidrio Technologies). Recordings were performed before and 40 min after either local perfusion of either TB21007 (100 nM) or control saline vehicle or systemic injection of TB21007 (1 mg/kg i.p.).

Radioligand binding and electrophysiological assays of recombinant receptors

The cDNAs encoding different rat and human $GABA_AR$ subunits (α1, α2, α3, α5, β2, β3 and γ2) were subcloned into the polylinker of the pcDNA3.1 vector (Invitrogen, USA) by standard techniques for transiently transfecting HEK293-F cells (ThermoFisher). Cells were transiently transfected with the plasmids containing the desired $GABA_AR$ subunit cDNAs (α, β, γ at a 1:1:1 ratio) using retro-inverso dioleoylmelittin (riDOM) 0.2 mg/nl (synthesized at Hoffman-La Roche) and PEI 25 kD 0.67 mg/ml. At 48 h post-transfection, the cells were harvested for membrane preparation and radioligand binding assays as described previously.[23] Briefly, the inhibition of 1 nM [^{3}H]-flumazenil binding by RO7015738 was measured in membranes expressing either α1β3γ2, α2β3γ2, α3β3γ2 or α5β3γ2 receptors. Non-specific binding was determined in the presence of 10 μM diazepam. Affinity values were calculated using Excel-Fit (Microsoft).

For electrophysiology studies, HEK293 cells stably expressing α1β2γ2, α2β3γ2, α3β3γ2 or α5β3γ2 receptor subtypes were obtained and maintained as previously described.[23] Cells were plated on glass coverslips, transferred to a chamber on the stage of a Nikon Diaphot 300 inverted microscope, and continuously superfused with a solution consisting of (in mM) 150 NaCl, 2.5 KCl, 1.2 $CaCl_2$, 1 $MgCl_2$, 10 HEPES and 30 sucrose, adjusted to pH 7.4. Glass electrodes (2-3 MΩ) were filled with a solution containing (in mM) 140 CsCl, 10 HEPES, 11 EGTA, 1 $CaCl_2$, 1 $MgCl_2$, 4 Mg-ATP and 25 sucrose, pH adjusted to 7.2 with CsOH. Whole-cell voltage-clamp recordings were performed at -60 mV using a MultiClamp 700A amplifier (Axon Instruments). GABA in the presence or absence of drugs was applied to the cell for 1 s in 1-min intervals using a multi-barreled micro-applicator (RSC-200, Biologic Science Instruments). For each experiment, at least 3 GABA control applications were generated, and only cells showing stable responses were selected for drug testing. Maximally effective concentrations of midazolam were applied for each $GABA_AR$ subtype as a positive control. Concentration-response curves were generated by applying increasing concentrations of each test drug to the same cell until a maximum response was observed (usually 2-3 times).

Computational modeling

Single neurons were modeled in the Neuron environment.[68] We used the morphology of a fully reconstructed layer 2/3 pyramidal neuron as well as voltage-dependent sodium, potassium, and HVA- and LVA-type calcium channels from prior modeling studies and based on electrophysiological recordings of cortical neurons.[69–72] A leak conductance with a reversal potential of -70 mV and a tonic GABAergic conductance with a reversal potential of -75 mV were also included. Model details are provided in ModelDB repository 2018023. To evaluate GABAergic modulation of dendritic calcium signals, an ~1 ms current (0.5-2.5 nA) was injected at the soma to evoke an action potential that propagated throughout the dendrite. ΔCa2+ was defined as the ratio of blocked to control integrated calcium channel current from 0-20 ms following the AP. Simulations were run in the presence and absence of the tonic GABAergic conductance.

QUANTIFICATION AND STATISTICAL ANALYSIS

All data are provided in the associated Data Spreadsheet. Analyses were performed using custom routines written in MATLAB (The Mathworks) and IgorPro (Wavemetrics). For quantification of resting tonic GABA currents, we plotted the distribution of holding current values before and after drug administration and fit these data to one-sided Gaussian curves.[18] The difference in peak locations of the two curves was taken as an estimate of the drug-sensitive tonic current. For quantification of SST-IN-evoked tonic currents, we calculated the difference in average membrane current for time windows immediately before and 300-400 ms or 650-750 ms

Please cite this article in press as: Chiu et al., SST interneurons facilitate dendritic calcium signaling via tonic activation of α5-GABA receptors, Neuron (2026), https://doi.org/10.1016/j.neuron.2026.04.017

(Figure 4) or 1150-1450 ms (Figure S4) after onset of optical stimulation. AP-evoked ΔCa^{2+} was calculated as the average ΔG/R over a 50 ms window, starting 5 ms after the stimulus. IPSC amplitudes were calculated by finding the peak of the evoked response and averaging the values within a 1 ms window. To assess DSI, we averaged IPSC amplitudes across 4 trials before and after induction. For analysis of in vivo data, regions of interest corresponding to active cell bodies and dendritic compartments were extracted automatically, followed by amplitude and frequency measurement using CaImAn, implemented in Python3.[73] Due to lack of vertical register for cell bodies and apical dendrites within V1, distinct compartments likely represented non-overlapping layer 2/3 neurons. Activity is highly synchronous within dendritic branches of the same cell, and we combined dendritic ROIs with correlation coefficients greater than 0.6 (Figure S3) for statistical validity.

For analysis of whole cell and synaptic currents under different conditions, we used a Wilcoxon matched-pairs test comparing data before and after drug application, with cell as the experimental unit. For analysis of *ex vivo* calcium transients, we used a random intercept linear mixed effects (LME) model in Matlab (fitlme) with spine as the experimental unit. Pharmacological treatment was considered a fixed effect, spine was considered a random effect (to account for the paired nature of the experiment), and cell was considered a random effect (to account for the nested nature of the experiments, with multiple spines sampled per cell). LME hypothesis testing was carried out using an F statistic and associated *p* value. Analysis of in vivo data was carried out by first averaging all amplitude and interval values within an animal, followed by Wilcoxon matched-pairs testing for before and after treatment, with animal as the experimental unit.